

# Extra sub-Doppler lines in the vicinity of the third-resonance $6S$ - $8P$ transition of atomic Cs attributed to optically induced Cs dimers

Thierry Passerat de Silans,<sup>\*</sup> Isabelle Maurin, Athanasios Laliotis, Pedro Chaves de Souza Segundo,<sup>†</sup> and Daniel Bloch<sup>‡</sup>

*Laboratoire de Physique des Lasers, Institut Galilée, Université Paris 13, Villetaneuse,  
UMR 7538 du CNRS, 99 Avenue J.B. Clément, F-93430 Villetaneuse, France*

(Received 21 January 2011; published 6 April 2011)

We report on the observation of additional sub-Doppler lines in a saturated absorption experiment when exploring the vicinity of the  $6S_{1/2} - 8P_{3/2}$  transition of Cs ( $\lambda = 388$  nm). These additional lines are observed only under a relatively strong irradiation of both the pump and the probe beams. Extra narrow lines are also observed in copropagating nonlinear spectroscopy, and around the lines of the V-type three-level system  $8P_{3/2} - 6S_{1/2} - 8P_{1/2}$  ( $\lambda_1 = 388$  nm,  $\lambda_2 = 389$  nm). We attribute these additional lines to a probing of high-lying molecular cesium, produced as a result of the optical excitation of Cs atoms, as the low Cs atom density ( $\leq 10^{12}$  cm<sup>-3</sup>) is unable to populate significantly the dimer states in the condition of thermal equilibrium.

DOI: [10.1103/PhysRevA.83.043402](https://doi.org/10.1103/PhysRevA.83.043402)

PACS number(s): 33.20.Xx, 32.80.Wr, 33.20.Kf, 82.20.Rp

## I. INTRODUCTION

The spectroscopy of alkali-metal vapors is very well known, and saturated absorption (SA) spectroscopy of alkali-metal vapors provides among the most valuable and easily identified narrow spectral references. It is hence a surprise when additional resonances appear on such reference spectra. However, when the optical irradiation is strong, and/or when the atomic density is relatively high, several phenomena, related to resonant nonlinear optical propagation, are susceptible to induce a spontaneous symmetry break [1]. It is also known that in the atomic vapor of an alkali metal, formation of molecules (alkali-metal dimers) may occur in a reversible manner, and that in dimer spectroscopy, richer than atomic spectroscopy, some resonances nearly coincide with those of atomic spectroscopy for the same species.

We report here on observations performed in the vicinity of the third-resonance line of Cs ( $6S \rightarrow 8P$ ), at 388 nm ( $6S_{1/2} - 8P_{3/2}$ ) and 389 nm ( $6S_{1/2} - 8P_{1/2}$ ). The experiment was initially implemented in view of getting atomic reference lines in the course of a selective reflection experiment [2]. The third-resonance line has an oscillator strength of  $\sim 10^{-3}$  (at 388 nm), the 389-nm line being much weaker ( $3 \times 10^{-4}$  [3]) due to the well-known Fermi anomaly of Cs [4]. The lifetime of Cs ( $8P$ ) ( $\sim 265$  ns) [5] is governed by a variety of decay channels, making the natural width of the transition as large as  $\sim 0.6$  MHz (note that a smaller value is mentioned in Ref. [6]).

A modest heating up of the Cs vapor—to increase atomic density—as well as focusing the beams, are required to obtain a saturated absorption spectrum owing to the weak oscillator strength of the considered line. Our experiments show that when the pump and probe are relatively intense, there are some additional (unreported) narrow lines inside the Doppler width, aside from the narrow saturated absorption components

from which the structure (Fig. 1) of the hyperfine manifolds of Cs ( $8P_{1/2}$ ) is resolved [ $A = 42.97 \pm 0.1$  MHz, ( $F = 3$ )–( $F = 4$ ): 172 MHz] and of Cs ( $8P_{3/2}$ ) [( $F = 2$ )–( $F = 3$ ): 23 MHz; ( $F = 3$ )–( $F = 4$ ): 30 MHz; ( $F = 4$ )–( $F = 5$ ): 37 MHz] [7]. Complementary experiments, performed with two independent lasers, lead to analogous observations in various experimental schemes, notably including copropagating geometries. Similar additional lines appear in nondegenerate three-level schemes, when the pump and probe beams are resonant for different transitions, starting from the two hyperfine levels of the ground state (separation 9.192 GHz), or even for different fine-structure components ( $6S_{1/2} - 8P_{3/2}$  and  $6S_{1/2} - 8P_{1/2}$ ). These observations help us to rule out the possibility to explain these observations by resonant nonlinear optics, and establish that these additional lines are of a spectroscopic origin, attributed to a selective population of molecular cesium induced by the strong light excitation, as the atomic density is unusually low to enable a notable dimer population at thermal equilibrium.

## II. EXPERIMENTAL SETUP

### A. Lasers

The experiments were conducted both with (i) a low-power ( $\sim 1$  mW) diode laser, operating with a specific chip (for 388–389 nm) mounted in an extended cavity (DL 100 from Toptica, see Ref. [2]), and (ii) the high-power ( $\sim 100$  mW) second-harmonic generation of the amplified emission of an extended cavity diode laser emitting at  $\sim 776$ – $778$  nm (SHG 110 from Toptica). For both sources, the overall linewidth was  $\leq 4$  MHz. Some imperfections are present in the initial spatial mode structure (due to the intrinsic modal asymmetry of “blue” laser chips, and to the nonlinear frequency doubling and amplification process as well), but the implementation of an optical filtering system (pinhole) did not modify any of our observations. For a better monitoring of the frequency scan, applied through piezoelements in the laser cavity, an auxiliary part of the laser beam is sent to a long and stable Fabry-Pérot frequency marker (free spectral range: 83 MHz). In spite of this, relatively large fluctuations ( $\sim 10$  MHz), which cannot be corrected, appear on long scans owing to acoustical noise and piezoelement nonlinearities.

<sup>\*</sup>Present address: Laboratório de Superfícies, Departamento de Física, Universidade Federal da Paraíba, Cx. Postal 5086, 58051-900 João Pessoa, PB, Brazil.

<sup>†</sup>Present address: Centro de Educação e Saúde, Universidade Federal de Campina Grande, Cuité-PB, CEP 58175-000, Brazil.

<sup>‡</sup>daniel.bloch@univ-paris13.fr

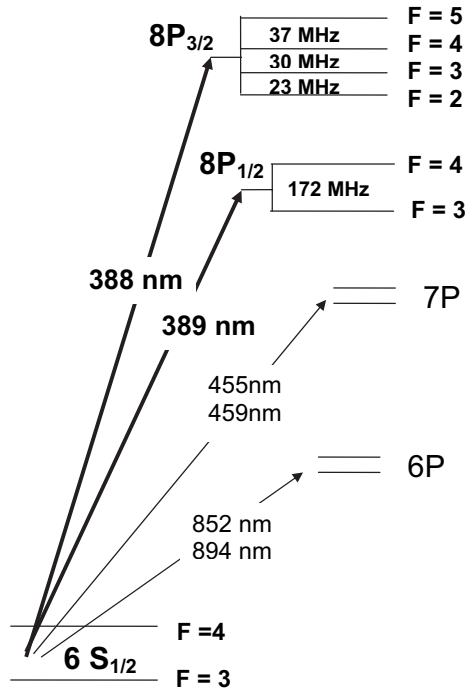


FIG. 1. Scheme of the relevant energy levels of Cs, and additional indication of the two first resonant levels.

### B. Cs vapor cells

Our experiments were performed on three different sealed Cs vapor cells. Two of them were glass cells, whereas the third one was made of sapphire windows and a copper body. These cells are heated up in an oven, allowing a control of the Cs density (for the density and temperature dependence, see, e.g., Ref. [8]). The observable differences between the various cells are essentially connected to differences in the absorption length (1–5 cm) of these cells, and this rules out effects associated with a cell contamination by impurities. In addition, the narrow linewidths obtained for the main lines of atomic saturated absorption confirm the absence of notable impurities.

### C. Experimental conditions

In a typical experiment, the pump beam is amplitude modulated (AM) with a mechanical chopper (occasionally with an acousto-optic modulator that enables a high modulation speed, but induces laser power losses), and the induced modulation on the counterpropagating probe beam is detected through a phase-sensitive amplifier. The pump and probe beams are either issued from the same laser—with a possible frequency shift between them, when an acousto-optic frequency shifter (typically at 80 or 200 MHz) is introduced—or they originate from two independent sources, of which only one is frequency scanned. Feedback is suppressed by optical isolators, and in most cases the beams bear a linear polarization, orthogonal to each other.

Both beams are focused in the cell (typical waist  $\sim 50$ – $100 \mu\text{m}$ ) to provide a relatively high intensity. In spite of the saturation, the absorption is non-negligible (typically up to 50%) due to the relatively high Cs density; the temperature is typically  $\sim 80^\circ\text{C}$  (atom density  $\sim 10^{13} \text{ cm}^{-3}$ ). The choice of

Cs density is not critical, as observations could be performed even at  $45^\circ\text{C}$  (atom density  $\sim 5 \times 10^{11} \text{ cm}^{-3}$ ) in a 5-cm-long cell. A too strong absorption precludes an effective overlap of the counterpropagating beams. Also, if the probe intensity is weak, or the Cs density low, only the usual (Doppler-free) components of saturated absorption are observed.

Complementary experiments with two independent lasers were also performed in a nearly copropagating geometry. The relevant spectroscopic parameter is thus the frequency difference between the two beams, while one beam is kept at a constant frequency and monitored in an auxiliary SA setup. In this geometry, there is often a remaining overlap of the two nearly copropagating beams, so that the probe beam is contaminated with a residual modulation of the pump beam. An additional frequency modulation (FM) on the probe beam allows the detection of the frequency-derived spectra, and enhances the narrow (sub-Doppler) components. A cascade demodulation (FM on the probe and AM on the pump) enables us to observe only the joint effect of the pump and of the probe

## III. EXPERIMENTAL OBSERVATIONS

### A. Experiments with a single laser or around a single atomic resonance

Additional sub-Doppler resonances, such as the ones shown in Fig. 2, are observed in the conditions of a standard saturated absorption experiment with the pump and probe beams issued from a single source, and require a relatively high intensity of the probe beam (typically  $\geq 5$ – $10 \text{ mW/mm}^2$  for the transition to the  $8P_{3/2}$  level), and high Cs density (typically  $\geq 10^{12} \text{ cm}^{-3}$  for the transition to the  $8P_{3/2}$  level). The intensity of the pump beam is also at least as large as  $5$ – $10 \text{ mW/mm}^2$ .

These resonances are characterized by the following features:

(a) Their typical width is 30–50 MHz : Although broader than the individual atomic saturated absorption hyperfine components, whose observed width is  $\sim 4$ – $6 \text{ MHz}$  (mostly due

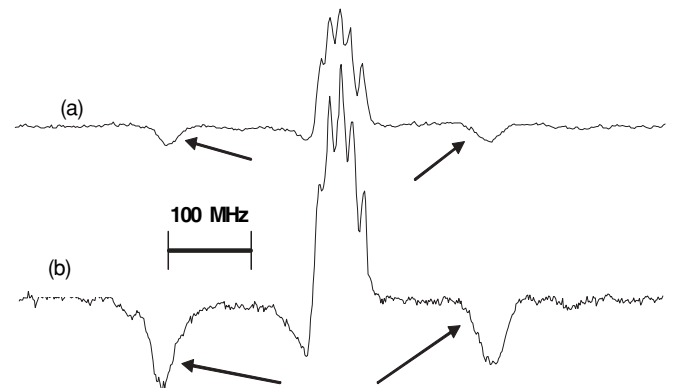


FIG. 2. Saturated absorption spectrum recorded in a counterpropagating geometry. Pump and probe beams originate from the same laser tuned around the  $6S_{1/2}$  ( $F=3$ )– $8P_{3/2}$  ( $F'=2,3,4$ ) Cs atomic transition. Pump intensity is  $\sim 50 \text{ mW/cm}^2$ . Probe intensity: (a)  $25 \text{ mW/cm}^2$ , (b)  $50 \text{ mW/cm}^2$ . The additional resonances are shown by arrows. The structure of the central resonance is due to the hyperfine structure of the Cs ( $8P_{3/2}$ ) level, and to the associated crossover resonances. The Cs vapor temperature is  $\sim 80^\circ\text{C}$ .

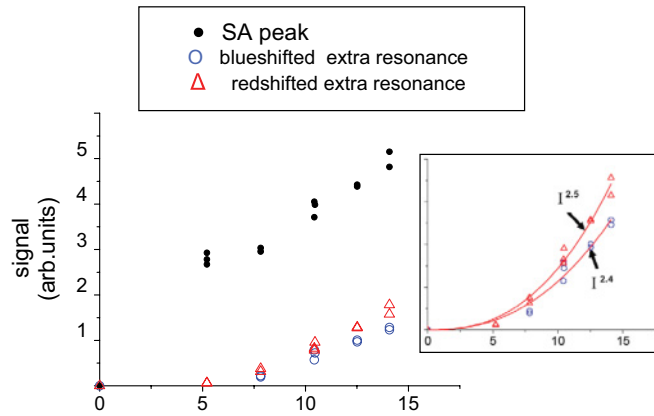


FIG. 3. (Color online) Amplitude of the peaks of the signals observed in a saturated absorption experiment (counterpropagating geometry) as a function of the probe intensity. The regular SA peak (filled circles) increases sublinearly with the probe intensity, owing to saturation effects, and in spite of a more efficient transmission. The amplitude of the additional resonances (open circles  $\circ$ ) for the blueshifted peak, triangles  $\triangle$  for the redshifted peak) increases nonlinearly with the probe intensity, with a fitting provided in the inset. In these experiments, the pump power is  $\sim 50$  mW/mm<sup>2</sup>.

to the laser linewidth), they remain clearly below the Doppler width (governed by  $ku_{\text{ther}} = (2\pi) 500$  MHz, with  $k = 2\pi/\lambda$ , and  $u_{\text{ther}}$  the most probable velocity).

(b) They remain clearly narrower than the overall hyperfine structure of the Cs ( $8P$ ) (see Fig. 1).

(c) Their amplitude compares with the main SA resonances (see Fig. 3). The influence of the polarization of the beams on the amplitude of these resonances is marginal.

(d) These sub-Doppler resonances most often correspond to an enhanced absorption (when the pump is on), while a standard SA atomic resonance corresponds to a reduced absorption (although the sign of the SA atomic resonances can be reversed in four-level processes, notably in the presence of optical pumping at a relatively high irradiation intensity).

(e) More additional resonances can appear under strong irradiation and density conditions (see Fig. 4). They can be located either between the first appearing set of additional resonances and the main SA resonances, or more remotely, but they remain in all cases inside the Doppler-broadened absorption.

(f) The position of these additional resonances, provided in Table I, is remarkably insensitive to the experimental conditions, although their amplitude is not. The shifts, relatively to the main SA atomic lines, differ according to the considered ground state [ $6S_{1/2}$  ( $F = 3$ ) or  $6S_{1/2}$  ( $F = 4$ )], and do not exhibit a significant red-blue symmetry.

Quantitatively, at the onset of their appearance, the amplitude of these additional resonances exhibits a strong nonlinear dependence on probe intensity (Fig. 3) and Cs density (Fig. 5).

In a SA experiment, an extra degree of flexibility is provided when introducing a frequency shift between the pump and the counterpropagating probe. This gives us the possibility to address various velocity groups, and is particularly susceptible to modify the relative amplitudes of crossover resonances, which are governed by the population of the probed velocity group. Here, such flexibility was provided either by an

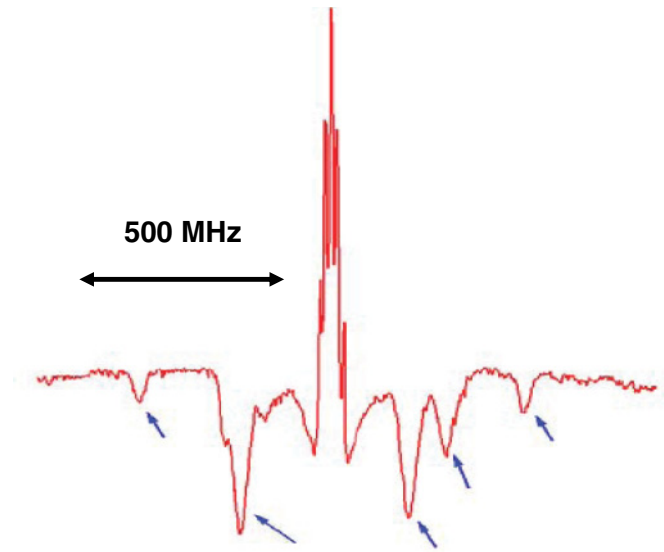


FIG. 4. (Color online) Same as Fig. 2, but for a relatively dense Cs vapor ( $9 \times 10^{12}$  cm<sup>-3</sup>, i.e.,  $\sim 50\%$  absorption), enabling the appearance of numerous additional resonances (marked by an arrow). The probe intensity is  $\sim 10$  mW/mm<sup>2</sup>.

acousto-optic shifter or, once a second laser has become available, by keeping one laser at a fixed frequency and scanning the other laser across the same resonance. In such experiments, equivalent to the experiment with a single frequency laser in a moving frame, we have observed that it is the whole spectrum that becomes frequency shifted, i.e., the additional resonances are shifted by the same amount as

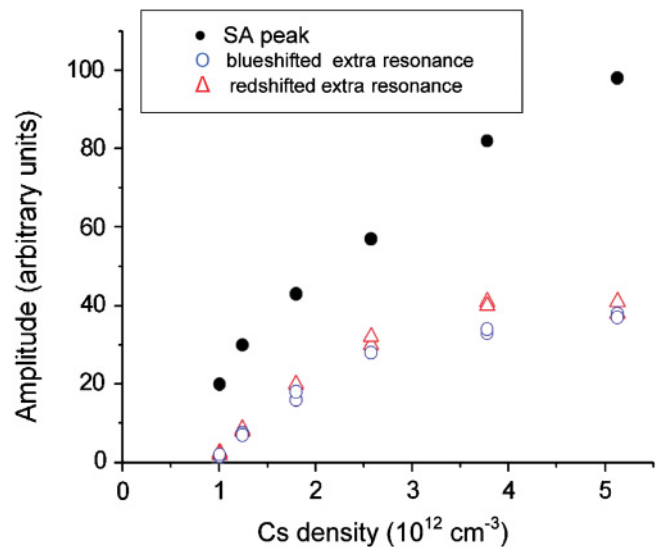


FIG. 5. (Color online) Amplitude of the peaks of the signals observed in a saturated absorption experiment (counterpropagating geometry) as a function of the Cs density. The regular SA peak (filled circles  $\bullet$ ) increases linearly with the Cs density. The amplitude of the additional resonances (open circles  $\circ$  for the blueshifted peak, triangles  $\triangle$  for the redshifted peak) increases nonlinearly with the Cs density: It starts with a power law with an exponent  $\sim 2-3$ , and quickly saturates owing to the absorption of the beams when the atomic density increases.

TABLE I. Frequency shifts of the additional resonances, relative to the cycling transitions  $F = 3 \rightarrow F' = 2$  or  $F = 4 \rightarrow F' = 5$  of the third-resonance component  $6S_{1/2} - 8P_{3/2}$ , as measured in a single laser experiment. The typical accuracy is  $\pm 10$  MHz. The most peripheral resonances are observed only for strong intensities and adequate densities.

Hyperfine ground state	Positions of the additional resonances				
$F = 3$	-425 MHz	-180 MHz	210 MHz	300 MHz	500 MHz
$F = 4$	-650 MHz	-355 MHz	310 MHz	-	-

expected for the main SA resonances. However, the relative amplitude of the additional resonances is affected, and for large frequency shifts between the pump and the probe, additional remote components can appear, located on the side for which the probe beam remains inside the Doppler width. Such additional resonances have been observed up to 1 GHz from the main SA atomic lines. All efforts to obtain additional resonances away from the domain of (Doppler-broadened) probe absorption yielded negative results.

### B. Experiments around nondegenerate three-level saturated absorption

Using the setup with two independent lasers, we have also performed nondegenerate velocity-selective three-level saturation spectroscopy, with the pump and probe frequencies shifted by  $\sim 9$  GHz, resonant to transitions starting from different hyperfine components of the ground state. In this case, “additional” resonances are also observed aside from the main three-level ( $\Lambda$ -type) saturation signal, in experimental conditions similar to those mentioned above (saturating intensities of both beams, relatively high atomic density). Analogous observations can even be performed in a V-type nondegenerate three-level scheme based upon the fine structure of the Cs ( $8P$ ) level, e.g., with the pump resonant on the  $6S_{1/2} \rightarrow 8P_{1/2}$  line (389 nm) and the probe resonant on the  $6S_{1/2} \rightarrow 8P_{3/2}$  line (388 nm).

The setup with two independent tunable lasers offers the versatility to study the copropagating geometry. Typically, one laser is kept at a constant frequency inside the Doppler-broadened absorption, and the other one is frequency scanned (across the same transition for a two-level SA signal, across a different one for a three-level scheme): Such a setup yields a spectrum revealing the hyperfine structure, independently of the velocity selected by the “pump” laser (assumed to be the laser at a fixed frequency, the detected probe laser being the frequency-scanned laser). The influence of the pump laser is limited to governing the height of the signal, according to the population of the selected velocity group, i.e., according to the position within the Doppler width. The same experimental conditions (i.e., vapor density and beam intensity) allowing for “additional” resonances in the counterpropagating geometry apply in the copropagating geometry (Fig. 6). These resonances exactly appear as an additional spectroscopic structure, i.e., as a remote addition to the hyperfine structure, whatever is the actual frequency chosen to be kept constant. Most often, their position appears consistent with those mentioned in Table I (once the required factor of 2 is introduced in the frequency scale, depending on whether a single or both beams are frequency scanned). In

some other cases, notably for a probing resonant to a transition starting from the  $6S_{1/2}$  ( $F = 3$ ) level—and the pump resonant to a transition starting from the  $6S_{1/2}$  ( $F = 4$ ) level—the position of the additional resonances differs from those observed in the counterpropagating geometry.

### C. Effect of a modulation

In all cases (counterpropagating or copropagating geometry, two- or three-level spectroscopic scheme), increasing the speed of the modulation applied to the pump beam leads to attenuated signals. This most probably indicates a process in which, at some step, the optical excitation induces optical pumping inside a long-lived level, as is the case when a hyperfine transfer  $F = 3 \rightarrow F = 4$  occurs in the  $6S_{1/2}$  ground state.

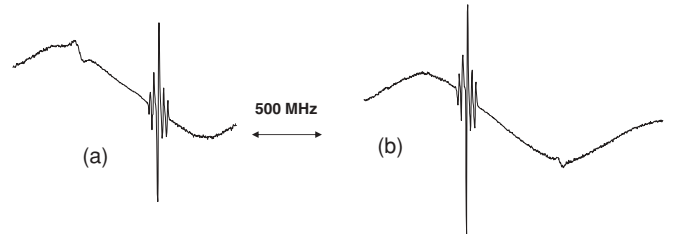


FIG. 6. FM transmission spectrum around the transition  $6S_{1/2}$  ( $F = 4$ )- $8P_{3/2}$  ( $F' = 3, 4, 5$ ), when a (nearly) copropagating pump beam is at a fixed frequency, within the Doppler line  $6S_{1/2}$  ( $F = 4$ )- $8P_{3/2}$ . Demodulation of the FM yields both the frequency derivative of the Doppler-broadened linear absorption, and the pump-probe signal. The dominant narrow resonance is when the probe and the pump are at the same frequency, i.e., the beams are resonant on the transitions to  $8P_{3/2}$  ( $F' = 3, 4, 5$ ) for respective velocities  $v_3, v_4, v_5$ . This provides a direct visualization of the pump-frequency shift: (a) pump frequency blueshifted relatively to the center of the line; (b) pump-frequency redshifted relatively to the center. Aside from the main resonance, the observed structure corresponds to the atomic hyperfine structure of Cs ( $8P_{3/2}$ ), as expected for a V-type three-level pump-probe scheme (e.g., for a pump-selected velocity  $v_3$ , probe resonant on the  $F' = 4$  or  $F'' = 5$  component). In (a), the narrow additional resonance on the left-hand side (red) is at a position approximately equivalent to the one found in counterpropagating geometry. In (b), under a strong redshift of the pump, a narrow additional resonance on the right-hand side (blue), falling within the probe Doppler absorption, becomes observable while the additional resonance seen in (a), which should be now located outside the Doppler-broadened line, is not observable anymore. Note that for these two-laser experiments, the (uncontrolled) frequency drift of the pump laser affects the overall spectral accuracy, in spite of the Fabry-Pérot monitoring of the probe beam frequency.



#### IV. ATTEMPTS AT INTERPRETATION

##### A. Nonlinear optics processes.

It has been known for a long time [1] that in the simple geometry of a SA experiment, intense counterpropagating beams are susceptible to induce strong nonlinear effects, leading to a spontaneous symmetry breaking. Such strong and resonant nonlinear effects can appear as narrow additional resonances inside the Doppler-broadened resonant width, corresponding to a combination of strong local nonlinearities—nonlinear dispersive effects, possibility of gain at some frequencies—with propagation in an optically thick medium (the possibility of a strong depletion through an absorption mechanism, and of an oscillation in directions specifically favorable to gain mechanism, etc.). Hence, modifying the propagation conditions, notably through a change of the atomic density, i.e., vapor temperature, or through the number of velocity-selected interacting atoms—controlled through the laser detuning—should severely affect the frequency position of the nonlinear Doppler resonant processes. In contrast, a major feature of our observations is the independence of the additional narrow (sub-Doppler) resonances relative to the experimental conditions. This is an essential point ruling out a possible interpretation of the observed additional resonances as the signature of a resonant nonlinear emission process. In the experiments with copropagating beams, a frequency shift within the Doppler width, applied to both beams, provides a simple way to modify the nonlinear propagation, but not the overlap between the two beams: It is hence particularly significant to note that the typical features of the spectrum (position of the additional resonances) do not appear affected by such a frequency shift.

##### B. Spectroscopy of dimers

The stability of the spectral structures that we observe (i.e., the distance between the additional resonances and the identified atomic transitions), whatever is the frequency of the pump beam within the Doppler width, is a good indication that the observed structures on the spectrum are truly of a spectroscopic origin. It is hence natural to look for spectral features associated to Cs dimers. Various spectral bands of Cs<sub>2</sub> were identified, and it has been noted for a very long time that there exist dimers transitions in the vicinity of the Cs 8S→8P line (388 and 389 nm) [9]. However, while an identification of dimers around the second resonance line of Cs was performed recently [10], the molecular energy levels in this region of the third-resonance line [11] have remained largely unexplored, most probably due to the lack of convenient sources, rendering very difficult the spectroscopic identification of a given line. In addition, the considered levels are too energetic to be reached efficiently by energy-pooling processes when optical excitation is limited to the first resonance line.

###### 1. Main features of dimer generation

Cesium dimers (Cs<sub>2</sub>) can be produced by collisions as well as photoassociation. In the conditions of thermal equilibrium, the cesium vapor is a mix of atomic and molecular vapor, but it is only when the temperature exceeds ~200 °C that a notable fraction (typically exceeding 1%) of the vapor consists

of dimers (from ground-state Cs atoms, three-body collisions are needed to sustain the generation of Cs<sub>2</sub>). It has also been noted that the efficiency of the dimer generation in a hot vapor can be modified through light irradiation, notably through an optical pumping mechanism inducing hyperfine redistribution in the ground state [12]. Alternately, via photoassociation of laser-cooled atoms, the relative number of Cs<sub>2</sub> dimers can be quite large in spite of the relatively low atomic density of cold Cs atoms [13]. Indeed, for cold atoms, the interaction between two atoms is much more efficient owing to an interaction time no longer limited by a fast relative (thermal) motion.

###### 2. Interpreting additional resonances as connected to the dimer spectrum

Although it is not unexpected that dimer lines are observed in close vicinity to atomic lines, the narrow additional resonances that we observe cannot be simply attributed to saturated absorption lines of the Cs<sub>2</sub> that already exist in the vapor at thermal equilibrium. Indeed, the temperature is so low that the Cs<sub>2</sub> density is surely a very small fraction of the atomic density: This is confirmed by the fact that with an extra diode laser operating in the infrared ~780 nm, it was only for a temperature higher than ~200 °C that we could observe (on the same setup) the relatively strong (i.e., requiring a relatively modest optical power) saturated absorption line of Cs<sub>2</sub>. Here, a quite low Cs density allows us to observe a signal height comparable to the atomic SA signal itself. Another major argument confirming that the observed additional resonances are not simply the saturated absorption signature of preexisting dimers, is that all attempts to observe some of these lines outside the Doppler resonance (our laser sources have a large tunability around 388 nm) have remained unsuccessful.

Dimer population is expected to depend nonlinearly upon the relevant atomic density, at least quadratically for a two-body process (note that the “relevant” density is not necessarily the total atomic density, and could include a kind of selection, in atomic excitation or velocity). Figure 5 shows a fast growth (nearly cubic for the first three points) of the amplitude of the additional resonances with atomic density. However, the absorption coming along with propagation in the Cs cell is non-negligible, so that this density parameter could not be modified without affecting other experimental parameters.

A remarkable point, already mentioned, is that the beam on which the detection is operated (“probe” beam) must be intense. This is unusual in spectroscopy, as it is ordinarily expected that the “probe” beam measures the linear absorption, or gain, of the medium, or its pump-induced modifications. This indicates that the additional resonances do not even originate in a saturated absorption process, in which the intense pump beam would both favor the production of dimers, and mark (i.e., velocity select) this population of dimers. The variety of possible processes explaining these additional resonances can include highly nonlinear spectroscopic process, such as a process relying on a Raman excitation performed by the two intense beams, followed by a linear spectroscopic probing. In particular, the copropagating geometry, with additional resonances observed for fixed frequency differences between the irradiating beams, resembles a Raman process, yielding Doppler-free resonances (conversely, for a

counterpropagating geometry, a standard Raman process is sensitive to the Doppler broadening). Extended information on the spectroscopic structure of molecular levels would then require a third laser, if the probed level is here populated only as the result of a Raman-induced dimer population. Such a scheme has been already considered and has provided novel spectroscopic data [14], but was never implemented with the near-UV wavelengths required for the considered dimer band.

### 3. Sub-Doppler width and velocity selection

As long as it appears that the additional resonances cannot be simply interpreted as a saturated absorption signal, it is worth discussing the narrow (sub-Doppler) width of the observed resonance. A remarkable feature of these additional lines is that they are not only sub-Doppler, but narrower ( $\sim 30$  MHz) than the hyperfine structure manifold of the atomic Cs ( $8P$ ) level: This is compatible with the fact that they are not of atomic origin. In the context of cold atoms, photoassociation leading to dimer formation is favored because the two atoms can interact for a very long time, owing to the cooling of the thermal motion. In contrast, for atoms in a thermal vapor, the usual velocity selection processes solely apply to an axial selectivity, while the duration of interaction between two atoms is limited by the thermal and unselected motion perpendicular to the light propagation axis. This makes it uneasy to ascribe the sub-Doppler features of these additional resonances to a velocity-selective process specifically required to induce the formation of dimers. Rather, among the multiple steps requiring a high intensity for both the pump and the probe, some of these processes, including optical pumping (see Sec. IIIC), are able to induce a (molecular) velocity selection. It may be also worth wondering if the atomic density—higher than for photoassociation of cold atoms—is not sufficient to allow a process that would be limited to relatively slow atoms

in the plane perpendicular to the beam axes (“slow” atoms corresponding to a Doppler width  $\sim 30$  MHz, i.e., the width of the additional resonances).

## V. CONCLUSION

We report on apparently unreported spectroscopic lines, observed in a very elementary spectroscopic setup, and this has motivated us to initiate a relatively systematic study. Because the investigation of a weak atomic line requires a relatively high light intensity, our experimental conditions favor nonlinear processes that could lead to the formation of molecular dimers, or even higher-order aggregates such as clusters. Moreover, the high level of excitation of Cs ( $8P$ ) allows complex step transfers through levels at an intermediate energy. The relatively high density of highly excited atoms allows the observation of molecular Cs at remarkably low overall atomic densities, without laser cooling technology. One of the intriguing results of these experiments is the sub-Doppler nature of the observed resonances, which is a possible indication of a high-order nonlinear process, combining selective formation of molecules and a standard nonlinear spectroscopy sub-Doppler process. A more systematic spectroscopic study would require a third independent laser beam, in order to allow a genuine spectroscopic probing (i.e., with a weak beam) of the molecular states produced in a complex nonlinear process.

## ACKNOWLEDGMENTS

P. Todorov and H. Failache (ECOS-Sud U08E01) have also participated in some steps of this work. We thank G. Pichler for stimulating discussions. We thank Thierry Billeton for the design of the Fabry-Pérot marker. This work was partly supported by INTAS South-Caucasus Project (Grant No. 06-1000017-9001).

- 
- [1] See, e.g., T. Honda, *Opt. Lett.* **18**, 598 (1993); N. B. Abraham and W. J. Firth, *J. Opt. Soc. Am. B* **7**, 951 (1990); L. A. Lugiato, G. I. Oppo, J. R. Tredicce, L. M. Narducci, and M. A. Pernigo, *ibid.* **7**, 1019 (1990); J. Pender and L. Hesselink, *ibid.* **7**, 1361 (1990); A. J. Scroggie and W. J. Firth, *Phys. Rev. A* **53**, 2752 (1996).
  - [2] P. Chaves de Souza Segundo, I. Hamdi, M. Fichet, D. Bloch, and M. Ducloy, *Laser Phys.* **17**, 983 (2007).
  - [3] F. S. Cataliotti, C. Fort, F. S. Pavone, and M. Inguscio, *Z. Phys. D* **38**, 31 (1976).
  - [4] O. Chun-Sing, G. F. Fülöp, O. Rédi, and H. H. Stroke, *J. Opt. Soc. Am.* **71**, 1072 (1981).
  - [5] A. Lingard and S. E. Nielsen, *At. Data Nucl. Data Tables* **19**, 533 (1977).
  - [6] Y. W. Liu and P. E. G. Baird, *Appl. Phys. B* **71**, 567 (2000).
  - [7] E. Arimondo, M. Inguscio, and P. Violino, *Rev. Mod. Phys.* **49**, 31 (1977); C. Tai, R. Gupta, and W. Happer, *Phys. Rev. A* **8**, 1661 (1973).
  - [8] A. N. Nesmeyanov, *Vapor Pressures of Chemical Elements* (Elsevier, New York, 1963).
  - [9] F. W. Loomis and P. Kusch, *Phys. Rev.* **46**, 292 (1934).
  - [10] M. Pichler, J. B. Qi, W. C. Stwalley, R. Beuc, and G. Pichler, *Phys. Rev. A* **73**, 021403(R) (2006).
  - [11] C. Vadla, V. Horvatic, and K. Niemax, *Phys. Rev. A* **80**, 052506 (2009).
  - [12] M. Allegrini, P. Bicchi, and S. Gozzini, *J. Chem. Phys.* **82**, 457 (1985).
  - [13] K. M. Jones, E. Tiesinga, P. D. Lett, and P. S. Julienne, *Rev. Mod. Phys.* **78**, 483 (2006), and references therein.
  - [14] A. M. Lyrra, H. Wang, T. J. Whang, J. C. Stwalley, and L. Li, *Phys. Rev. Lett.* **66**, 2724 (1991).